Chapter 3

The Performance of Insulation and Arc Interruption of the Environmentally Friendly Gas CF_3I

Dengming Xiao

Additional information is available at the end of the chapter

http://dx.doi.org/10.5772/intechopen.79968

Abstract

Many researches of trifluoroiodomethane (CF_3I) have shown that CF_3I has many excellent properties that make it one of the possible alternatives of SF_6. This paper reveals the effect laws of CF_3I gas content, gap distance, gas pressure, polarity, and electric field nonuniform coefficient on the insulation performance of CF_3I gas mixtures. In general, CF_3I-N_2 gas mixtures present a superior dielectric strength than CF_3I-CO_2 under different electric field sets. The experimental results indicate that 20 and 30% content CF_3I-N_2 gas mixtures can achieve nearly 50 and 55% insulation strength of pure SF6. In addition, to evaluate the arc interruption performance of environmentally friendly gas CF_3I, we set up a CF_3I transient nozzle arc model to study its thermodynamic and transport property. The analysis shows that CF_3I gas has a good arc interruption capability, which mainly functions thermodynamic and transport properties approach that of SF_6, and some are even better than SF_6. The decomposition process is also aggravated by impurities including metal and water. The main by-products are greenhouse gases with GWP below that of SF_6 and are lowly toxic and incombustible.

Keywords: gas insulation, environmentally friendly gases, CF_3I

1. Comparison of CF_3I and its mixtures with SF_6 and its mixtures on insulation property

In order to assess the insulation strength of CF_3I and its mixtures, power frequency breakdown voltages of SF_6 and 20%SF_6–80%N_2 mixture are measured in the same experimental condition [1]. The result is shown in **Tables 1** and **2**.

Gas	U_{SF_6} (kV)				$U_{20\%SF_6-80\%N_2}$ (kV)			
d (mm)/*P* (MPa)	0.3	0.2	0.15	0.1	0.3	0.2	0.15	0.1
5	126.8	82.0	60.7	34.9	82.2	53.7	39.0	25.3
10	222.3	150.2	112.9	82.9	170.5	112.6	82.5	57.7
15	315.0	220.1	174.8	120.0	246.0	166.7	123.9	90.7

Table 1. Power frequency breakdown voltages of SF_6 and 20%SF_6–80%N_2 gas mixtures in slightly nonuniform electric field.

Gas	U_{SF_6} (kV)				$U_{20\%SF_6-80\%N_2}$ (kV)			
d (mm)/*P* (MPa)	0.3	0.2	0.15	0.1	0.3	0.2	0.15	0.1
5	44.0	42.6	30.0	21.5	34.4	24.7	18.6	14.8
10	56.4	74.4	64.1	47.9	69.6	53.1	41.6	30.1
15	64.1	95.2	93.4	72.4	91.3	79.0	61.5	44.5
20	72.4	111.0	120.3	97.0	110.1	102.3	82.4	59.4

Table 2. Power frequency breakdown voltages of SF_6 and 20%SF_6–80%N_2 gas mixtures in highly nonuniform electric field.

Seen from **Table 1**, when P = 0.1 MPa and d = 10 mm, breakdown voltage of SF_6 in slightly nonuniform electric field is 82.9 kV, approximate to the standard value of breakdown voltage in uniform electric field, 89 kV/(mm•MPa). Moreover, breakdown voltage of 20%SF_6–80%N_2 mixture is 57.7 kV, roughly 70% of the value of SF_6, which is in agreement with data of other researchers.

Figure 1 compares the insulation property of CF_3I-N_2 gas mixtures [2] with SF_6 and SF_6-N_2 gas mixtures in slightly nonuniform electric field. It is obvious that the breakdown voltage of CF_3I-N_2 mixture is lower than SF_6 and SF_6-N_2 in the whole pressure range and distance range but higher than N_2 in the same condition. **Table 3** shows the insulation strength of CF_3I-N_2 mixture relative to pure SF6 and 20%SF_6–80%N_2 mixture in different distances and pressures. It can be known from **Table 3** that the insulation strength of 20%CF_3I–80%N_2 in slightly nonuniform electric field is as high as 50% of SF_6 and 70% of 20%CF_3I–80%N_2. If the mixing ratio of CF_3I increases to 30%, the insulation strength of CF_3I-N_2 mixture becomes 55% of SF6 and 78% of 20%SF_6–80%N_2. In this paper, CF_3I-CO_2 mixture, whose insulation strength is 97% of CF_3I-N_2 in the same condition if the mixing ratio is 30%, is researched [3]. With this proportion relationship, insulation property of CF_3I-CO_2 mixture relative to SF_6 and 20%SF_6–80%N_2 can be calculated [4].

About the situation in highly nonuniform electric field, breakdown voltage of CF_3I-N_2 mixture with the distances of 10 mm and 20 mm as examples is compared with SF_6 and 20%SF_6–80%N_2, as shown in **Figure 2**. Because of the strong electronegativity of SF_6 and CF_3I, the mixtures present drastic changing breakdown property. It is useless to define the relative insulation strength in highly nonuniform electric field generally, and analysis according to specific pressure condition is necessary [5].

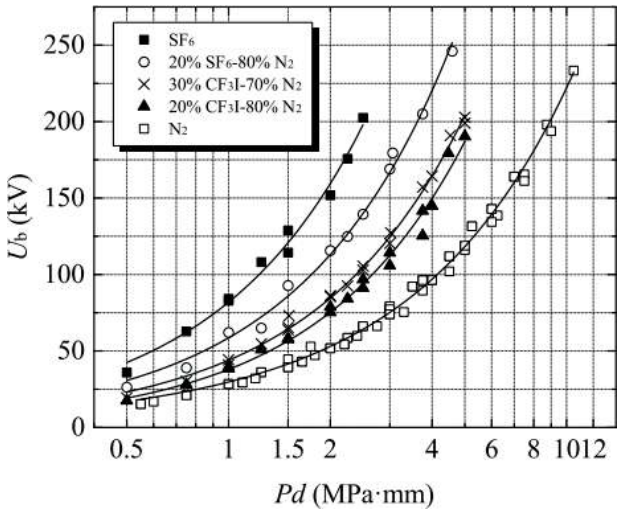

Figure 1. Comparison of the insulation property of CF_3I-N_2 mixture with SF_6 and SF_6-N_2 mixture in slightly nonuniform electric field.

***P* (MPa)**	**0.3**	**0.2**	**0.15**	**0.1**	**0.3**	**0.2**	**0.15**	**0.1**
d (mm)	$U_{20\%CF_3I-80\%N_2}/U_{SF_6}$				$U_{20\%CF_3I-80\%N_2}/U_{20\%SF-80\%N_2}$			
5	0.53	0.49	0.49	0.50	0.82	0.75	0.77	0.67
10	0.54	0.52	0.51	0.48	0.70	0.70	0.70	0.69
15	0.57	0.52	0.48	0.49	0.73	0.69	0.68	0.64
d (mm)	$U_{30\%CF_3I-70\%N_2}/U_{SF_6}$				$U_{30\%CF_3I-70\%N_2}/U_{20\%SF_6-80\%N_2}$			
5	0.58	0.55	0.58	0.55	0.89	0.84	0.85	0.76
10	0.57	0.57	0.57	0.54	0.75	0.76	0.77	0.77
15	0.61	0.57	0.55	0.55	0.78	0.77	0.78	0.72

Table 3. Insulation strength of CF_3I mixture relative to SF_6 and 20%SF_6–80%N_2 in slightly nonuniform electric field.

Seen from **Figure 2**, power frequency breakdown voltage of SF_6 has obvious "hump effect" as a function of pressure with the distance of 10 and 20 mm. Similarly, the increase of breakdown voltage of 20%-mixed SF_6-N_2 mixture with pressure also tends to saturate. It is discovered by comparison that 30%CF_3I–70%N_2 possesses comparative insulation property to 20%SF_6–80%N_2, which is around 60% of SF_6. When P = 0.2 MPa, the insulation property of 30%CF_3I–70%N_2 mixture is as high as 80% of 20%SF_6–80%N_2 mixture and more than 55% of pure SF_6 [6]. When the pressure increases to 0.3 MPa, breakdown voltage of SF_6 declines rapidly because of the "hump effect." In this way, the breakdown voltage of 30%CF_3I–70%N_2 gas mixtures even exceeds pure SF_6, becoming 1.17 times higher than the latter. Because the power frequency breakdown voltage of 20%SF_6–80%N_2 always increases with the pressure, insulation strength

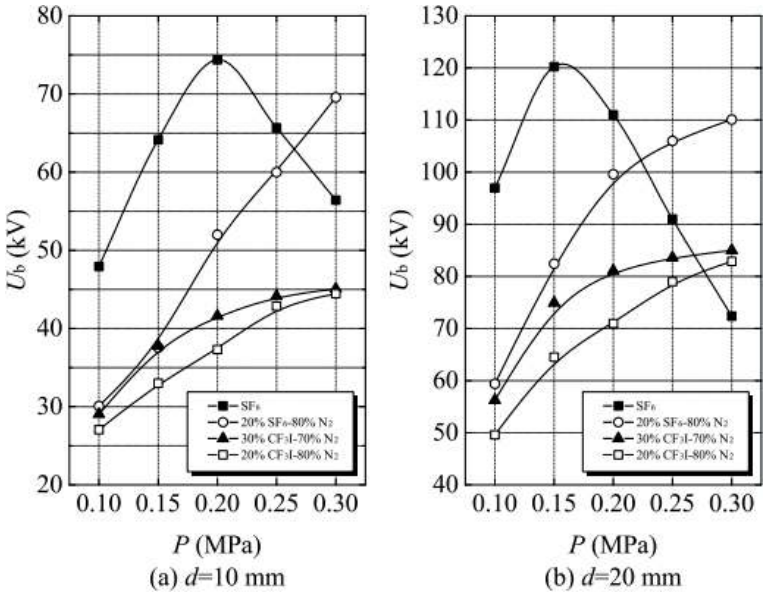

Figure 2. Comparison of the insulation property of CF_3I-N_2 gas mixtures with SF_6 and SF_6-N_2 mixture in highly nonuniform electric field.

of 30%CF_3I–70%N_2 is only around 75% of 20%SF_6–80%N_2 [7]. It can be indicated that the insulation strength of CF_3I-N_2 gas mixtures relative to SF_6-N_2 declines gradually with the increase of pressure, but the breakdown level is always more than 55% of SF_6. It is partly because the "hump effect" of SF_6 in the pressure is 0.1–0.3 MPa and also because interfusing buffer gas N_2 improves the abnormal breakdown phenomenon in highly nonuniform electric field [8]. **Table 4** shows the insulation strength of CF_3I gas mixtures relative to SF_6 and 20%SF_6–80%N_2 in the same condition. It can be seen that the insulation property of 20%CF_3I–80%N_2 in highly nonuniform electric field is more than 49% of SF_6 and 69% of 20%SF_6–80%N_2 in the same condition.

CF_3I-CO_2 gas mixtures, also affected by "hump effect," present obvious decline in high pressure. Under the pressure 0.1 and 0.15 MPa, the breakdown voltage of 30%-mixed CF_3I-CO_2 gas mixtures is 60% of pure SF_6 and 1.05 times of 20%SF_6–80%N_2 gas mixtures [9]. However when the pressure rises to 0.3 MPa, the insulation property of CF_3I-CO_2 gas mixtures is only around 40% of 20%SF_6–80%N_2 mixture [10]. Relative insulation strength of different pressures is shown in **Table 4** in detail.

The insulation properties of CF_3I-N_2 and CF_3I-CO_2 gas mixtures can be concluded with the analysis above.

In uniform electric field, the insulation strength of 30%-mixed CF_3I-N_2 gas mixtures can approach 72% of pure SF_6 theoretically and in slightly nonuniform electric field more than 55% of pure SF_6 [11]. In highly nonuniform electric field, the relative insulation strength of

d (mm)	10	20	10	20
P (MPa)	$U_{30\%CF_3I-70\%N_2}/U_{SF_6}$		$U_{30\%CF_3I-70\%N_2}/U_{20\%SF_6-80\%N_2}$	
0.10	0.61	0.58	0.97	0.95
0.15	0.59	0.62	0.91	0.91
0.20	0.55	0.73	0.77	0.79
0.30	0.80	1.17	0.75	0.77
P (MPa)	$U_{20\%CF_3I-80\%N_2}/U_{SF_6}$		$U_{20\%CF_3I-80\%N_2}/U_{20\%SF_6-80\%N_2}$	
0.10	0.56	0.51	0.90	0.84
0.15	0.51	0.54	0.79	0.78
0.20	0.49	0.64	0.68	0.69
0.30	0.79	1.15	0.69	0.75
P (MPa)	$U_{30\%CF_3I-70\%CO_2}/U_{SF_6}$		$U_{30\%CF_3I-70\%CO_2}/U_{20\%SF_6-80\%N_2}$	
0.10	0.64	0.62	1.02	1.02
0.15	0.62	0.59	1.05	0.86
0.20	0.55	0.42	0.77	0.46
0.30	0.67	0.59	0.55	0.39

Table 4. Insulation strength of CF_3I gas mixtures relative to SF_6 and $20\%SF_6$–$80\%N_2$ gas mixtures in highly nonuniform electric field.

CF_3I-N_2 gas mixtures is influenced by the pressure seriously, which ranges from 55 to 117% in the researched pressure range [12].

The insulation strength of 30%-mixed CF_3I-CO_2 gas mixtures can approach 68% of pure SF_6 theoretically in uniform electric field, and in slightly nonuniform electric field, it can be more than 53% [13]. In highly nonuniform electric field, the relative insulation strength is also influenced by the pressure. The insulation strength of 30%-mixed CF_3I-CO_2 gas mixtures is 0.42–0.62 times of pure SF_6.

Detailed comparative data and the insulation strength of $20\%SF_6$–$80\%N_2$ gas mixtures are listed in **Table 5**. Seen from the table, whether in slightly nonuniform electric field or highly nonuniform electric field, the insulation strength of CF_3I-N_2 is better than CF_3I-CO_2 in the same condition. Therefore, in actual equipment application, CF_3I-N_2 gas mixtures with the mixing ratio of 20–30% should be considered preferentially.

Then, principles of applying CF_3I mixture in actual electrical equipment are discussed with the example of 40.5 kV cubicle-type gas-insulated switchgear (C-GIS).

C-GIS, vulgarly named "gas-filled cabinet," is suitable for situations that have high requirement on reliability and limited space and floor area such as rail transit, high buildings, and industrial enterprises. 40.5 kV C-GIS is the most popularly employed. Known from the survey

Gas	Electric field	U_{CF_3I-X}/U_{SF_6}	$U_{CF_3I-X}/U_{SF_6-N_2}$
	Uniform	0.72	0.88
30%CF_3I–70%N_2	Slightly nonuniform	0.55	0.78
	Highly nonuniform	0.55–1.17	0.75–0.97
	Uniform	0.68	0.83
30%CF_3I–70%CO_2	Slightly nonuniform	0.53	0.75
	Highly nonuniform	0.42–0.67	0.39–1.02

Table 5. Insulation strength of CF_3I gas mixtures relative to SF_6 and 20%SF_6–80%N_2 gas mixtures.

of products on the market, the most popular practice currently is employing SF_6 with the pressure 0.12–0.15 MPa (abs) as the main insulation medium of primary loop. For example, the SF_6 charge pressures of XGN46–40.5 model C-GIS developed by Xi'an High Voltage Apparatus Research Institute and ZX2 model C-GIS produced by ABB are, respectively, 0.15 and 0.13 MPa. Meanwhile, some companies employ higher pressure, e.g., 8DA10 model C-GIS produced by Siemens, whose SF_6 charge pressure is 0.26 MPa. C-GIS is complicated on structure and different on shape, containing function units such as breakers, disconnectors, current/voltage transformers, etc., and forming both slightly nonuniform electric field and highly nonuniform electric field. In accordance to relative insulation strength shown in **Table 5**, replacing SF_6 in C-GIS with CF_3I-N_2 with the mixing ratio of 20–30% as insulation medium without changing the gap distance and pressure, insulation strength is not strong enough, so it is necessary to adjust the charge pressure or structure properly.

Through analysis, we can know that increasing pressure or increasing gap distance can effectively improve the insulation level of CF_3I gas mixtures. If the gap distance is kept constant, the CF_3I-N_2 gas mixtures of 20–30% mixing ratio at 0.25–0.3 MPa will reach the insulation level of SF_6 at 0.15 MPa. In this case, there is no need to change the existing C-GIS internal structure; only a thickened metal enclosure is needed to ensure the operation pressure and the leakage level meet the requirements. At the same time, the liquefaction temperature of CF_3I-N_2 gas mixtures around this pressure can be maintained below −25°C, which is in accordance with the requirements of GB/T 11022-2011 on the operating temperature of the switch equipment. If the operating pressure is kept constant, the data in **Figure 1** and **Table 1** show that to achieve the same insulation strength as SF_6, the gap distance of 30%CF_3I–70%N_2 gas mixtures needs to be increased by about twice as much.

Therefore, although the insulation strength of the CF_3I gas mixtures is weaker than pure SF_6, CF_3I gas mixtures can not only achieve the same insulation level as the SF_6, but also the liquefaction temperature can meet the operation requirement of the switch equipment by adjusting the operating condition or structure parameters properly. More importantly, CF_3I-N_2 gas mixtures will not affect global warming. It can solve the unfriendly environmental problems of SF_6 and realize the green upgrading of electrical equipment. Therefore, it is suggested that CF_3I-N_2 gas mixtures with the mixing ratio of 20–30% can be used as alternative medium for SF_6 in low- and medium-voltage electrical equipment.

Based on the results of power frequency and lightning impulse tests, it is shown that the insulation strength of CF_3I-N_2 gas mixtures increases with the increase of CF_3I mixing ratio in slightly nonuniform electric field or in highly nonuniform electric field. For CF_3I-CO_2 gas mixtures, the breakdown voltage varies with the mixing ratio in slightly nonuniform electric field, similar to CF_3I-N_2. However, in highly nonuniform electric field, the breakdown voltage of 10%-mixed CF_3I-CO_2 gas mixtures is higher than mixtures with mixing ratio of 20 and 30%, due to the abnormal breakdown of the high pressure. It can be seen that higher mixing ratio of electronegative gas in the CF_3I gas mixtures does not always cause better insulation performance, and it will also be influenced by many factors such as the gap distance, the pressure, and the unevenness of the electric field.

From the change of the breakdown voltage with the gap distance, the breakdown voltage of CF_3I-N_2 and CF_3I-CO_2 gas mixtures increases linearly with the increase of the gap, and the increase speed is proportional to the pressure in slightly nonuniform electric field. In highly nonuniform electric field, the breakdown voltage of CF_3I-N_2 gas mixtures shows a tendency to saturate with the gap distance, while the CF_3I-CO_2 combination has obvious nonlinear characteristics.

From the change of the breakdown voltage with the pressure, the insulation strength of the CF_3I-N_2 and CF_3I-CO_2 gas mixtures in the slightly nonuniform field increases linearly with the increase of the pressure and even shows a certain degree of negative synergy. However, under the highly nonuniform electric field environment, there is a clear "hump" in the power frequency breakdown voltage of CF_3I-CO_2 gas mixtures with the change of pressure, and the positive lightning impulse coefficient in the "hump" section is always less than 1.

From the effect of polarity on discharge, the breakdown voltage of CF_3I gas mixtures under positive polarity is higher than that of negative polarity in slightly nonuniform electric field. But in highly nonuniform electric field, the opposite is true. In addition, the uniformity of electric field will also affect the insulation performance of CF_3I gas mixtures. Therefore, in the actual product application, the uniformity of the electric field should be improved as much as possible for the purpose to ensure that the insulation strength of the CF_3I gas mixtures can be maintained at a high level.

Finally, by comparing with the SF_6 and 20%SF_6–80%N_2, it is found that the 20%CF_3I–80%N_2 gas mixtures can reach the insulation level of 50% of pure SF_6 gas and about 65% of 20%SF_6–80%N_2 gas mixtures. When the mixing ratio of CF_3I is increased to 30%, insulation strength of CF_3I-N_2 gas mixtures can reach about 55% and 75% of SF_6 and 20%SF_6–80%N_2 gas mixtures, respectively. For the combination of CF_3I-CO_2, 30%-mixed CF_3I-CO_2 gas mixtures can reach the insulation level of more than 53% of pure SF_6 in slightly nonuniform electric field, but in highly nonuniform electric field, relative insulation strength depends on the pressure and can only reach 42–67% of the latter.

2. The radial temperature distribution characteristics and leading energy transport process of CF_3I nozzle arc

The transient temperature distribution of arc is decided by the mutual equilibrium among the energy input of arc, different energy transport processes, and changing rate of energy storage,

which determines the characteristics of arc in turn. We analyze the arc extinction characteristics of CF_3I through the thermodynamic characteristics of CF_3I arc.

The temperature of arc plasma changes with the changes of time and position, and that's decided by the interactions of the produce of the joule heat of arc and different energy transport processes in itself. The following are the calculation and analysis of the energy balance of the core area (in the radius with 83.3% highest temperature) and conducting regions (in the radius with 4000K temperature) of arc in the conditions with 900 A large current, 50 A small current, and current-zero period.

By the radial temperature analysis of arc, during the process that the head of the moving contact moves from the nozzle upstream to the throat, because the space of the throat is small, and the moving contact and thermal plasma of arc will block the flow of the fluid to the catchment area through the nozzle, and the slow speed of the fluid causes a bigger radius of arc so that the core area is not obvious and the temperature is relatively lower. We choose the time of 900 A current to analyze in **Table 6**. In the time of large current, the sinusoidal current waveform changes relatively slowly with the change of time, and the changing rate of energy storage of the core area of arc can almost be negligible, and as the slow decline of arc, global energy of arc also goes down, so the change of energy storage in the radius of arc reaches more than 20%. As the interior of the thicker arc cannot be influenced by the cold fluid, the electric power produced in the core area of arc is lost more than 90% by the radiation process, and beyond the core area of arc, the interactions of arc and fluid are more drastic, and the energy loss of radiation lowers obviously. As a whole, the axial convection process of arc does positive work, and the core area does less work. Although the radial convection of arc is small, it takes the joule heat away, and that's because the cold fluid in upstream moves from the entrance to the lower right and contacts with the thermal plasma with a bigger oblique angle to form convection, especially the cold fluid which flows along the slope of fixed contact even forms eddy in the interior of arc. Therefore, the radial convection in the arc boundary has a good cooling effect, especially in the reabsorption area of the radiation energy.

When the current lowers to 50 A, the moving contact moves to the catchment of nozzle, and the distance of contact reaches more than 18 mm. The throat of the nozzle opens completely, and the thermal characteristics of the nozzle arc are decided by the energy distribution and transport process in **Table 7**. Differing from large current, because of the temperature distribution

Arc boundary	Electric power input (10^3W)	Radiation loss (%)	Radial thermal conductance (%)	Axial thermal convection (%)	Radial thermal convection (%)	Energy loss of pressure to do work (%)	Changing rate of energy storage of electric power (%)
Boundary of core area (R_{833})	4.185	−93.9	−14.0	13.6	−11.2	−0.1	2.4
Arc boundary (R_{4k})	4.768	−25.8	−52.6	25.8	−68.7	0.2	21.9

Table 6. Percentage of electrical power input associated with various energy transport processes for the whole CF_3I arc length at core and arc boundary at 900 A.

Arc boundary	Electric power input (10^3W)	Radiation loss (%)	Radial thermal conductance (%)	Axial thermal convection (%)	Radial thermal convection (%)	Energy loss of pressure to do work (%)	Changing rate of energy storage of electric power (%)
Boundary of core area (R_{833})	4.179	−46.6	−69.4	17.8	−6.2	−10.5	11.7
Arc boundary (R_{4k})	5.666	−0.1	−79.4	−25.7	21.0	−16.2	4.7

Table 7. Percentage of electrical power input associated with various energy transport processes for the whole CF_3I arc length at core and arc boundary at 50 A.

characteristics of arc and the effect of high-speed cold fluid, the loss ratio of radiation energy decreases sharply. After the reabsorption process of radiation in the arc boundary, the loss ratio of radiation energy approaches zero. Around arc, the high-speed movement of the cold fluid in the nozzle makes arc form an obvious high-temperature core area. The fast change of radial temperature makes the radial thermal conduction become strong, and the energy transport ratio in the core area and arc area is both 70%. In comparison, the convection effect works little to the change of energy. Because the moving contact pulls to the right and arc plasma strengths in axial, the axial convection does positive works in the core area of arc, but in the arc boundary, the high-speed cold fluid around arc effectively takes the energy away, and it has an obvious cooling effect to arc. The radial convection in the core area begins to do negative works, and that's because the temperature gradient in the core area of arc is very big, and the gas with relatively lower temperature in the radiation reabsorption region begins to enter into the core area to maintain the conservation of mass in the interior of arc; however, out of the core area of arc, the decline of the radial temperature becomes slow, and the radial convection effect still does positive works.

In the current-zero area, shown in **Table 8**, the joule heat of arc is zero, and the temperature of plasma lowers to less than 10,000 K, and the radiation effect is almost 0. The radius of arc

Arc boundary	Electric power input (10^3W)	Radiation loss (%)	Radial thermal conductance (%)	Axial thermal convection (%)	Radial thermal convection (%)	Energy loss of pressure to do work (%)	Changing rate of energy storage of electric power (10^3W)
Boundary of core area (R_{833})	0	−0.1	−13.3	−35.8	−50.4	−2.4	1.796
Arc boundary (R_{4k})	0	−0.0	−19.0	−37.4	−48.7	−1.8	1.841

Note: Because the current input in the current-zero area is zero, the change of arc's energy storage is the changing power of energy, and it is regarded as the energy input to measure the strength of every energy transport process.

Table 8. Percentage of electrical power input associated with various energy transport processes for the whole CF_3I arc length at core and arc boundary at current zero.

is very small, and the thermal conduction is relatively weaker. Convection mainly consumes arc's energy, whether in the core area or within the arc boundary, and the radial thermal convection takes more than 30% energy away as the axial reaches about one half of the change of arc's energy.

3. The arc's characteristics near the arc-zero area

The thermal interruption of nozzle arc is decided by the arc's temperature around the current-zero area. Through the discussion of the above section, when it's close to the current-zero area (25 A and lower), the arc's temperature and radius decrease rapidly and become a key time of arc interruption, and this process is worth being researched more. When the current is very small, a strong radial thermal conduction makes arc form a relatively bigger radial temperature gradient in the radiation reabsorption area, which takes the energy in the arc's interior away effectively. And this promotes more entrance of cold fluid of outside into the high-temperature plasma of arc (to maintain the conversation of mass), so that the radial convection heat dissipation becomes the main form of energy transport when the current approaches zero. The superposition of two effects explains the sharp declines of the arc's temperature and radius in dozens of microseconds before current zero-crossing in **Figures 3** and **4**.

The changes of nozzle throat arc's temperature and radius with time near current-zero area are shown in **Figures 3** and **4**. They show that in 30 s before arc-zero area, CF_3I arc's temperature shows a trend of faster decrease without obvious phenomenon that the declines of temperature about time decrease. And the arc's radius decreases with time. From the characteristic

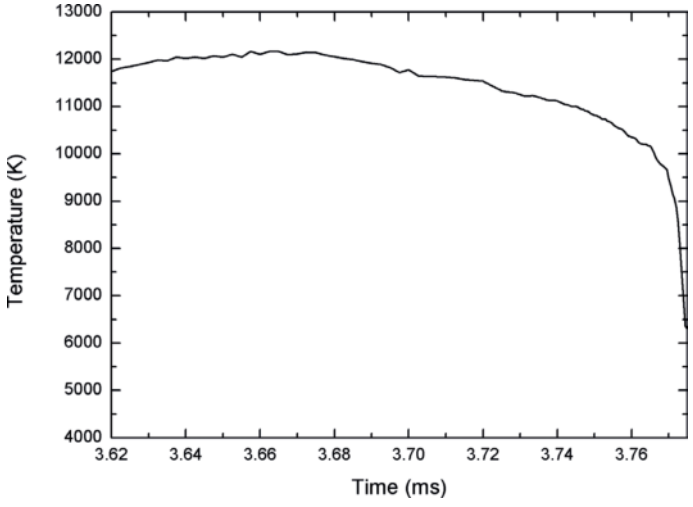

Figure 3. Arc temperature varied with time at nozzle throat near current zero.

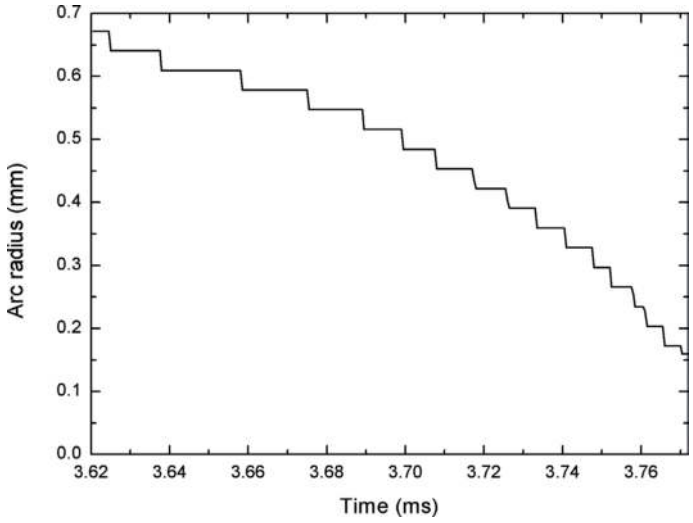

Figure 4. Arc radius varied with time at nozzle throat near current zero.

	About arc's radius	About arc's temperature
10 μS before current zero-crossing	24.75 μs	40.64 μs
Current-zero area	3.90 μs	2.27 μs

Table 9. Characteristic time of CF_3I arc near current zero.

time of arc (see **Table 9**), at 10 μs before current zero-crossing (arc current is about 5 A), the characteristic time about arc's radius and temperature is 24.75 and 40.64 μs which are equivalent to SF_6 arc's values in the same time. In the last 10 μs, the characteristic time of CF_3I arc in the current-zero area lowers to about 3 μs which is much smaller than air and CO_2 arc and approaches SF_6 arc. The comparison shows that the declines of CF_3I arc's temperature and radius near current-zero area are equivalent to SF_6 and much bigger than air and CO_2 arc.

4. Analysis of the by-product after CF_3I interrupts arc

There are three reasons to cause gas decomposition, and they are decomposition caused by electron collision, thermal decomposition, and photodecomposition. There are mainly first two types in the high-voltage electrical equipment. The main discharge forms in switching arc or equipment such as GIS are high-power arc discharge, spark discharge, and partial discharge. Among them, high-power discharge has large current and a long time of duration, and energy can accumulate in a short time, and temperature can reach more than 20,000 K, and it's the most serious discharge form of decomposition reaction.

Although physical parameters of CF_3I show good thermal interruption characteristics, the same with SF_6, it will have decomposition reaction in the conditions of high temperature and high gas pressure. Though most decomposition reactions are reversible reaction, after arc interrupt, there are still some by-products to be produced. These by-products will influence subsequent quenching of arc, and their toxicity and environmental characteristics will influence the application of CF_3I in switching arc equipment. This section does spectrum analysis to the arc-later gases, combining the calculating results of the thermomotive equilibrium state gas composition, and evaluates the types of arc-later by-products of CF_3I and the possible influence from the impurities.

4.1. Spectrum analysis to the arc-later compositions of CF_3I

The arcing experiment is done in the SF_6 switch cabinet with nominal voltage of 12 kV and nominal current of 630 A, and we use the sine-input arc current of effective value of 400 and 630 A. We conduct sampling of the arc-later gas of CF_3I after five times' arcing experiment. The experimental gas is CF_3I with purity of more than 99.5% which has known impurities of CO_2 and CF_3Br and water with volume ratio lower than 18 ppm (1.8×10^{-3}%). Before the experiment, we have done the insulation test and moisture content test to the switch cabinet to ensure that it can reach experimental standard.

Gas detection uses PLOT-Q chromatogram column to separate and detect the gas, and the detection is done 48 hours after sampling of gas. We use the cleansed needle tubing for sampling and put into the detection equipment for automatic detection, gas separation, and spectrum distinction. Spectrometer has a distinguishing uniformity of more than 80% to the gas composition, and we can trust the judgment of gas composition. As needle tubing sampling will inevitably mix with air, being a mass of N_2 and trace amounts of CO_2, we will find N_2 and CO_2 in the detection. Every gas sample is about 10 μL.

Arc-later gas composition gotten by spectral testing is shown in **Table 10**. In the experiment, 400 A current successfully interrupts for five times, but 630 A current restrikes in the first interruption experiment and continues to burn for dozens of milliseconds. Therefore, arcing

	Original gas	400 A five times	630 A one time
N_2	√	√	√
CF_4	√	√	√
CO_2	√	√	√
C_2F_6		√	
CHF_3	√	√	
H_2O	√	√	√
C_4F_8	√	√	
CF_3I	√	√	√

Table 10. Gas composition after arc for CF_3I arc obtained through mass spectrum measurement.

experiment under 630 A current is just done for one time, and we obtain the gas after unsuccessful interruption as testing sample. In the results, except the main composition CF_3I, other impurities or gas decompositions are N_2, CF_4, CO_2, C_2F_6, CHF_3, H_2O, and C_4F_8. N_2 and H_2O are impurities because of mixture of air. CO_2, CHF_3, and C_4F_8 exist in the original gas, so they are the impurities in the producing process of gas. Therefore, CF_4 and C_2F_6 are the products of the high-voltage and large-current arcing experiment of CF_3I. The comparisons of the response values of CF_3I, CF_4, C_2F_6, C_4F_8, and CHF_3 in original gas and after different times' arcing experiment are shown in **Figure 5**.

From the spectrum data of CF_3I, CF_3I decomposes little after five times' successful interruption of 400 A arc, and CF3I is 97.0% of original gas; the decomposition can be ignored. But after the unsuccessful interruption of 630 A current, CF_3I is only 3.4% of original gas. Other gases' spectrum data shows that under conditions of successful interruption, only 3% CF_3I produces CF_4 and C_2F_6 and little C_4F_8 and CHF_3 as the gas reaches room temperature from arc's high temperature. According to conservation of elements, it will separate out a little iodine. When the arcing interruption fails, more than 95% CF_3I becomes CF_4 and separates out iodine at the same time. This shows that the ratio of by-product after successful arcing interruption of CF_3I is very low and the main by-products are CF_4 and C_2F_6. However, when arc interruption fails and arc continues to burn, a mass of CF_3I will decompose and produce much CF_4 so that it cannot be used as arc-quenching medium. By examining the switch cabinet after the failure of arc quenching, we can find that there are much black solid attached on the surface of insulator and contact and this solid is carbon and iodine. The production of elementary substance shows that during the drastic burning of arc-restrike gas, many organic compounds decompose into elementary substance due to the lack of oxidizer (such as oxygen). Therefore, when CF_3I is applied in interrupting arc, we should reserve enough margin for interrupting current, and at the same time, we can use some absorbents or make air-blast-arc method to eliminate produced iodine.

4.2. Characteristic analysis of CF_3I decomposing products

Based on environmentally friendly purpose and toxicity, we analyze the composition of arc-later gases, and the results are listed in **Table 11**. It shows that compared with SF_6, the global warming potential (GWP) of decomposing gases of CF_3I under conditions of large current decreases at different levels. Except CF_4, the existence time in the atmosphere of other gases drastically reduces. As for toxicity, the arc-later decompositions of CF_3I belong to perfluorocarbon and partial fluorocarbon, which both have low toxicity, so it will cause headache, nausea, or dizziness under conditions of long-time or high-density inhalation. While doing experiment, we should note ventilation and appropriate self-protection.

In a word, after CF_3I arc discharges under conditions of high voltage and large current, main by-products are perfluorocarbons, CF_4 and C_2F_6; in the event of mixing trace amounts of water, it will produce a little hydrofluorocarbons such as CHF_3 and C_2HF_5. Perfluorocarbon and hydrofluorocarbon with few carbon atoms both have low toxicity; the consequences of inhalation are connected with the density. Only in closed environment, when human inhales higher-density gas, it will damage the cardiovascular system to a certain degree. During experiment and use, we should note ventilation and appropriate self-protection to ensure a safe process.

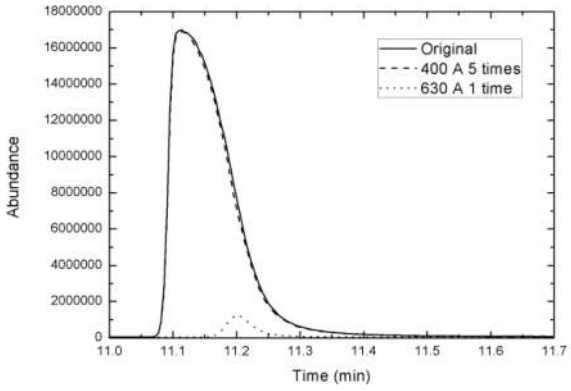
Original
400 A 5 times
630 A 1 time
Abundance
Time (min)

(a)

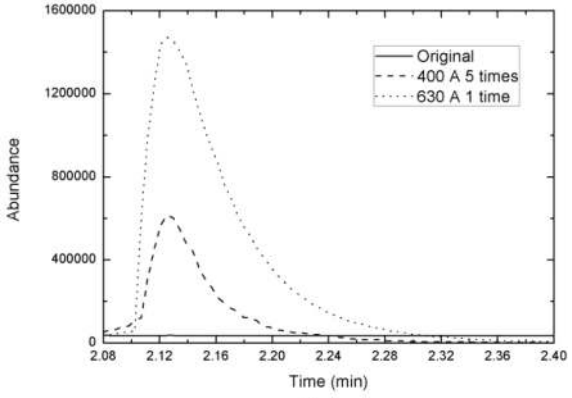
Original
400 A 5 times
630 A 1 time
Abundance
Time (min)

(b)

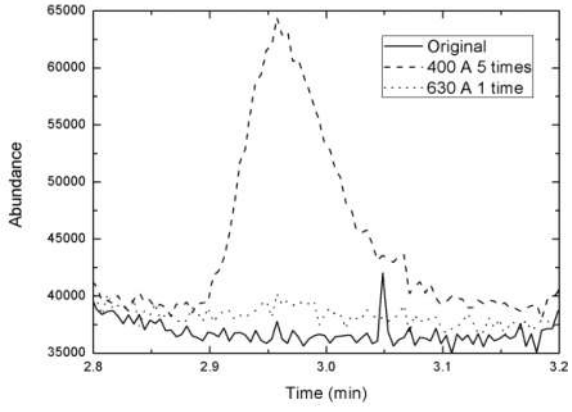
Original
400 A 5 times
630 A 1 time
Abundance
Time (min)

(c)

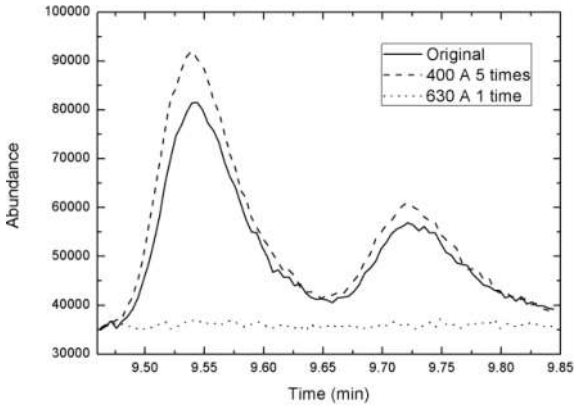

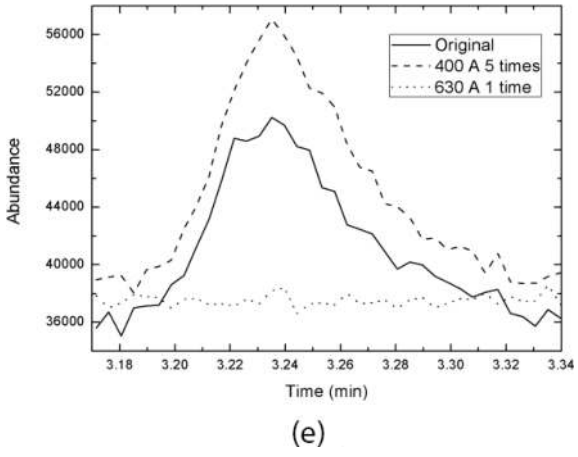

Figure 5. Mass spectrum data of CF_3I gas composition after arcs: (a) CF_3I, (b) CF_4, (c) C_2F_6, (d) C_4F_8, and (e) CHF_3.

Gas	Dielectric strength compared with SF_6	Liquefaction temperature (°C)	GWP	Existence time in the atmosphere (year)	Toxicity
C_2F_6	0.78–0.79	−78	9200	10,000	Low toxicity
CF_4	0.39	−186.8	6500	50,000	Low toxicity
CHF_3	0.18	−78.2	11,700	264	Low toxicity
C_2HF_5	0.59	−48.5	14,800	32.6	Low toxicity

Table 11. Environmental and toxic analysis of CF_3I gas composition after arc.

5. Conclusions

1. After adjustment to operation conditions or structure size of the electrical equipment, CF_3I gas mixtures can reach equivalent insulation level of SF_6, and at the same time, the liquefaction temperature can satisfy operation conditions of switch equipment. Because CF_3I-N_2 gas mixtures will not influence global warming, it can resolve environmentally unfriendly problems and realize the green upgrade of the electrical equipment. Therefore, we suggest that 20–30% CF_3I-N_2 gas mixtures can be applied as SF_6 alternatives in medium- and low-voltage electrical apparatus.
2. CF_3I has a good arc interruption characteristic, and before current zero-crossing, it approaches SF_6, and some thermodynamic properties are even better than SF_6. CF_3I decomposes easily after large-current arcs, high-temperature decomposing products are hard to recombine after arc extinction, and they are easy to be influenced by impurities such as water and so on and produce a little hydrofluorocarbon. Few-carbon-atom perfluorocarbon and hydrofluorocarbon both have low toxicity, so we should take appropriate actions such as absorbent or gas mixtures to eliminate or restrain decomposing products.

Acknowledgements

This work is supported by the National Natural Science Foundation of China (Grant No.51337006).

Author details

Dengming Xiao

Address all correspondence to: dmxiao@sjtu.edu.cn

Department of Electrical Engineering, Shanghai Jiao Tong University, Shanghai, China

References

[1] Taki M, Maekawa D, Odaka H, Mizoguchi H, Yanabu S. Interruption capability of CF_3I gas as a substitution candidate for SF_6 gas. IEEE Transactions on Dielectrics and Electrical Insulation. 2007;**14**:341-346

[2] Cressault Y, Connord V, Hingana H, Teulet P, Gleizes A. Transport properties of CF_3I thermal plasmas mixed with CO_2, air or N_2 as an alternative to SF_6 plasmas in high-voltage circuit breakers. Journal of Physics D: Applied Physics. 2011;**44**:495202

[3] Wang W, Rong M, Wu Y, Yan JD. Fundamental properties of high-temperature SF_6 mixed with CO_2 as a replacement for SF_6 in high-voltage circuit breakers. Journal of Physics D: Applied Physics. 2014;**47**:255201

[4] Liu J, Zhang Q, Yan J, Zhong J, Fang M. Analysis of the characteristics of DC nozzle arcs in air and guidance for the search of SF_6 replacement gas. Journal of Physics D: Applied Physics. 2016;**49**:435201

[5] Zhang X, Dai Q, Han Y, et al. Investigation towards the influence of trace water on CF_3I decomposition components under discharge. High Voltage Technology. 2016;**42**:172-178

[6] Yokomizu Y, Ochiai R, Matsumura T. Electrical and thermal conductivities of high-temperature CO_2–CF_3I mixture and transient conductance of residual arc during its extinction process. Journal of Physics D: Applied Physics. 2009;**42**:215204

[7] Yokomizu Y, Ochiai R, Matsumura T. Particle composition of CO_2-CF_3I mixture at temperatures of 300-30,000 K. The Transactions of the Institute of Electrical Engineers of Japan B. 2007;**127**:1281-1286

[8] Qiu Y. GIS Equipment and Its Insulation Technologies. Beijing: China Water & Power Press; 1994

[9] Xiao S, Cressault Y, Zhang X, Teulet P. The influence of Cu, Al, or Fe on the insulating capacity of CF_3I. In: Physics of Plasmas (1994-present), vol. 23. 2016. p. 123505

[10] Christophorou LG, Olthoff JK, Green DS. Gases for Electrical Insulation and Arc Interruption: Possible Present and Future Alternatives to Pure SF6. NIST TN-1425, vol. 82011. p. 391

[11] Deng Y. Fundamental research of the application of environmentally friedly insulation gas CF_3I in the electrical equipment [PhD thesis]. Shanghai: Shanghai Jiao Tong University; 2016

[12] Christophorou LG. Insulating gases. Nuclear Inst & Methods in Physics Research A. 1988;**268**:424-433

[13] Zhao X. The research of arc extinguishing and insulation characteristics of environmentally friendly insulation gas CF_3I [PhD thesis]. Shanghai: Shanghai Jiao Tong University; 2018